Abrupt $PbTiO_3/SrTiO_3$ superlattices grown by reactive molecular beam epitaxy

J. C. Jiang, X. Q. Pan,[a] and W. Tian
Department of Materials Science and Engineering, The University of Michigan, Ann Arbor, Michigan 48109-2136

C. D. Theis and D. G. Schlom
Department of Materials Science and Engineering, Penn State University, University Park, Pennsylvania 16802-5005

(Received 18 June 1998; accepted for publication 11 March 1999)

$PbTiO_3/SrTiO_3$ superlattices were grown on (001) $SrTiO_3$ substrates by reactive molecular beam epitaxy (MBE). Sharp superlattice reflections were observed by x-ray diffraction. High-resolution transmission electron microscopy of a $[(PbTiO_3)_{10}/(SrTiO_3)_{10}]_{15}$ superlattice revealed that the $PbTiO_3/SrTiO_3$ interface structure is atomically sharp. The superlattice interfaces are fully coherent; no misfit dislocations or other crystal defects were observed in the superlattice by transmission electron microscopy. Selected area electron diffraction patterns indicated that the $PbTiO_3$ layers are oriented with the *c* axis parallel to the growth direction. The dimensional control and interface abruptness achieved in this model system indicate that MBE is a viable method for constructing oxide multilayers on a scale where enhanced dielectric effects are expected. © *1999 American Institute of Physics.* [S0003-6951(99)02919-8]

Ferroelectric and dielectric superlattices have been extensively studied in recent years, due to their scientific importance and technological promise.[1–7] Fabrication of such superlattice structures, particularly when controlled on an atomic-layer level, can explore predictions of giant dielectric constants[8,9] over a wide temperature range[9] and be used to fabricate new functional devices, e.g., those involving a designed grading of composition in one direction on an atomic scale.[10,11] Just as the ability to fabricate semiconductor superlattices with unit cell precision enabled the investigation and exploitation of many new electronic and photonic devices, so too should the ability to assemble ferroelectric and dielectric materials at will be expected to lead to improved fundamental understanding of ferroelectric coupling and improved devices that utilize ferroic effects. Lead titanate, $PbTiO_3$, together with its solid solutions, is a candidate compound for making superlattices with promising properties. Calculations suggest that a $Pb(Zr,Ti)O_3/SrTiO_3$ multilayer with layer thicknesses in the 46–140 Å range will exhibit giant dielectric response over a broad temperature range.[9]

Lead titanate is a perovskite with a cubic structure above its Curie temperature (T_C) of 490 °C.[12] Below T_C, $PbTiO_3$ is ferroelectric with a tetragonal unit cell, lattice constants $a=3.904$ Å and $c=4.152$ Å at room temperature, and a distortion (c/a ratio) of 1.063.[12] It is difficult to grow superlattices containing $PbTiO_3$ ferroelectric layers due to the volatility of lead. $PbTiO_3$ and $SrTiO_3$ mixtures form a solid solution over their entire composition range.[13] Thus, $PbTiO_3/SrTiO_3$ superlattices are metastable; it is energetically favorable for the two materials to dissolve into each other, forming a solid solution. In the present work, superlattices of $PbTiO_3$ and $SrTiO_3$ layers have been fabricated by reactive molecular beam epitaxy (MBE) and their interfaces investigated by high-resolution transmission electron microscopy (HRTEM). The interfacial abruptness and superlattice coherence exceed those of previously reported superlattices containing $PbTiO_3$.

The MBE experimental setup is described elsewhere.[14] In short, molecular beams of the constituent elements are supplied to the film surface from thermal sources. Purified ozone is used as the oxidant, which is supplied to the film via a directed inlet nozzle. The $SrTiO_3$ is deposited by the sequential deposition of SrO and TiO_2 monolayers as shown in Fig. 1, where each monolayer dose of strontium is controlled by feedback from an atomic absorption spectroscopy monitor and each titanium monolayer is supplied using feedback from reflection high-energy electron diffraction (RHEED) intensity oscillations.[15] The $PbTiO_3$ layers are deposited using adsorption-controlled growth conditions. An excess of lead (~3 times greater than the titanium incident flux) is supplied to the surface of the film while the titanium is supplied in monolayer doses, as shown in Fig. 1. A detailed description of the adsorption-controlled MBE growth of $PbTiO_3$ has been reported elsewhere.[16] For the growth of the superlattice described below, the substrate temperature is maintained at 580 °C and the ozone background pressure is maintained at 2×10^{-5} Torr.

The $PbTiO_3/SrTiO_3$ superlattice described was grown on a $SrTiO_3$ (001) substrate that was etched with a buffered-HF solution prior to growth, exposing a TiO_2-terminated surface.[17] The thickness of the $PbTiO_3$ and $SrTiO_3$ layers in the superlattice was controlled to be ten unit cells, i.e., the

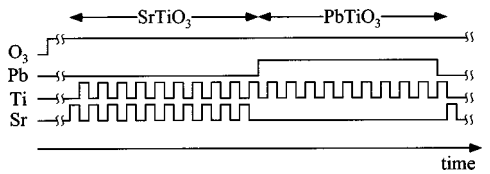

FIG. 1. Timing diagram showing the flux supplied from the molecular beams as a function of time for the growth of the $PbTiO_3$ and $SrTiO_3$ layers of the $[(PbTiO_3)_{10}/(SrTiO_3)_{10}]_{15}$ superlattice.

[a]Corresponding author. Electronic mail: panx@umich.edu

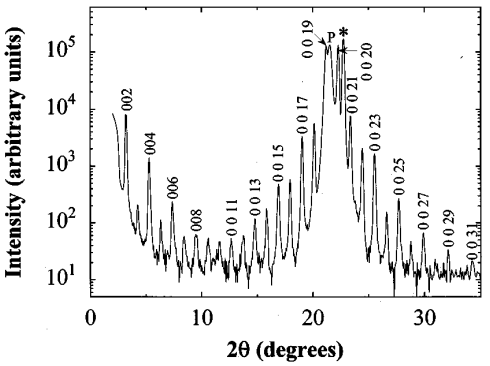

FIG. 2. A θ-2θ x-ray diffraction scan of the multilayer containing the $[(PbTiO_3)_{10}/(SrTiO_3)_{10}]_{15}$ superlattice. The 00l reflections of the superlattice are labeled, P denotes the location of the 001 reflection of the thick $PbTiO_3$ layers, and the 001 reflection of the $SrTiO_3$ substrate is marked by an asterisk (*).

target thicknesses of the $PbTiO_3$ and $SrTiO_3$ layers were 41 and 39 Å, respectively (assuming bulk lattice constants). The target thickness of the entire superlattice was 1200 Å (15 repeats). The structure of the superlattice can be described as $[(PbTiO_3)_{10}/(SrTiO_3)_{10}]_{15}$. Before growing this superlattice, a buffer layer consisting of a 1000 Å thick La-doped $SrTiO_3$ layer followed by a 500 Å thick $PbTiO_3$ layer was grown on the $SrTiO_3$ substrate. On top of the $[(PbTiO_3)_{10}/(SrTiO_3)_{10}]_{15}$ superlattice, another thin $PbTiO_3$ layer was grown.

Figure 2 shows a θ-2θ four-circle x-ray diffraction scan of the heterostructure. Sharp 00l superlattice reflections are clearly visible and indicate excellent regularity of the periodic structure. The superlattice constant (83.7 ± 0.2 Å, determined using a Nelson–Riley[18] analysis of the 00l reflections) is slightly longer than the attempted period of 80.5 Å. This discrepancy indicates either a slight error in the strontium or titanium doses supplied to the film or a deviation of the lattice constants of these materials from their bulk values when fabricated as ultrathin layers.

For HRTEM analysis, cross-sectional slices were obtained by cutting the $PbTiO_3/SrTiO_3$ heterostructures along the [010] direction of $SrTiO_3$ and then gluing the film surfaces of the slices face to face. Cross-sectional HRTEM specimens were prepared by mechanical grinding, polishing, and dimpling, followed by Ar-ion milling at 5 kV. HRTEM studies were carried out within a JEOL-4000 EX microscope operating at 400 kV, which has a point resolution of 0.17 nm.

A cross-sectional view of the heterostructure is shown in Fig. 3(a). The layers in the image from bottom to top correspond, respectively, to the $SrTiO_3$ substrate, the 1000 Å thick La-doped $SrTiO_3$ and 500 Å thick $PbTiO_3$ buffer layer, the $[(PbTiO_3)_{10}/(SrTiO_3)_{10}]_{15}$ superlattice, and the final $PbTiO_3$ thin layer. A selected area electron diffraction (SAED) pattern taken from the area including the lower $PbTiO_3$ and La-doped $SrTiO_3$ buffer layers is shown in Fig. 3(b), which was recorded with the electron beam direction parallel to the [100] zone axis of the $SrTiO_3$ substrate. It is identified to be a superposition of a [100] zone SAED pattern of cubic $SrTiO_3$ and a [100] zone SAED pattern of tetragonal $PbTiO_3$. The elongated shape of diffraction spots in the diffraction pattern indicates that the a and b axes of tetragonal $PbTiO_3$ lie in the plane of the interface and that the c axis lies

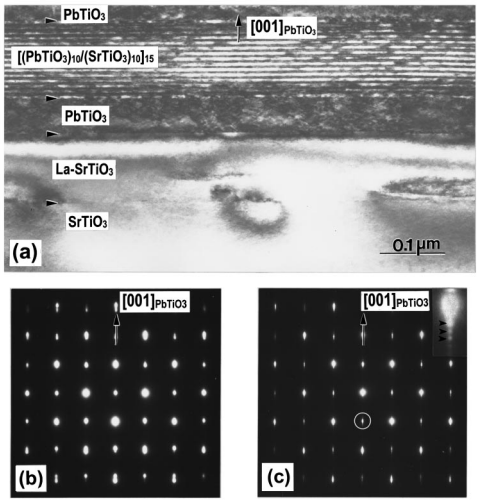

FIG. 3. (a) Bright-field TEM image showing the cross-sectional structure of the $PbTiO_3/SrTiO_3$ multilayer. (b) A SAED pattern taken from the area including the La-doped $SrTiO_3$ and $PbTiO_3$ layers beneath the superlattice. (c) A SAED pattern from the $[(PbTiO_3)_{10}/(SrTiO_3)_{10}]_{15}$ superlattice region; the inset shows an enlargement of the circled reflection.

parallel to the growth direction. This conclusion is also true for the thin $PbTiO_3$ layer above the $[(PbTiO_3)_{10}/(SrTiO_3)_{10}]_{15}$ superlattice according to the HRTEM studies.

In the superlattice region of Fig. 3(a), layers with higher intensities (bright) and lower intensities (dark) correspond to the $SrTiO_3$ and $PbTiO_3$ layers, respectively. A constant thickness is seen for each of the individual layers. The corresponding SAED pattern of the $[(PbTiO_3)_{10}/(SrTiO_3)_{10}]_{15}$ superlattice structure is shown in Fig. 3(c), which is taken with the electron beam direction parallel to the [100] axis of the $SrTiO_3$ substrate. Equally spaced satellite reflections corresponding to a periodicity of ~80 Å along the growth direction are seen in the inset, which is an enlarged view of the circled spot in Fig. 3(c).

Figure 4(a) is a HRTEM image of the $[(PbTiO_3)_{10}/(SrTiO_3)_{10}]_{15}$ superlattice. The individual $PbTiO_3$ and $SrTiO_3$ layers show highly perfect single crystalline structures. The c axis $PbTiO_3$ thin layers in the superlattice region have the parallel to the growth direction. The tetragonality (c/a ratio) of the $PbTiO_3$ layers is about 1.06, measured from the HRTEM images.

A Fourier-filtered HRTEM image of the interface between $PbTiO_3$ and $SrTiO_3$ from the superlattice region is shown in Fig. 4(b). It clearly shows different image characteristics between the $PbTiO_3$ and $SrTiO_3$ layers. Figure 4(c) shows a profile of the image intensities along the marked line in Fig. 4(b). The intensity of the bright spots undergoes a sharp change at the interface. From this study it can be deduced that the structural width of the $PbTiO_3/SrTiO_3$ interface is about one unit cell.

In $PbTiO_3$ based heteroepitaxial thin films, tetragonal $PbTiO_3$ layers may be either a-axis or c-axis oriented, with frequent twinning (i.e., 90° domain boundaries).[19,20] In the $[(PbTiO_3)_{10}/(SrTiO_3)_{10}]_{15}$ superlattice region of the film studied, the $PbTiO_3$ layers have a tetragonal structure, are c-axis oriented, and are free of twin boundaries. The formation of such a superlattice structure can be understood as follows. At the growth temperature of 580 °C both structures are cubic, with bulk lattice constants of 3.967 Å for $PbTiO_3$

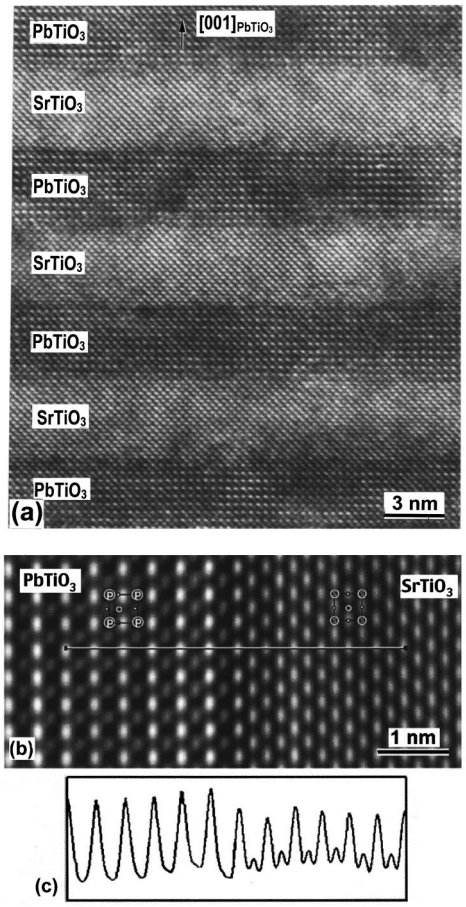

FIG. 4. (a) A HRTEM image of the $[(PbTiO_3)_{10}/(SrTiO_3)_{10}]_{15}$ superlattice structure taken with the electron beam parallel to the [100] axis of $SrTiO_3$. (b) Fourier-filtered HRTEM image of the $[(PbTiO_3)_{10}/(SrTiO_3)_{10}]_{15}$ superlattice. (c) A profile of the image intensity from the area marked in (b).

and 3.929 Å for $SrTiO_3$.[21] The lattice strain between the $SrTiO_3$ and $PbTiO_3$ thin layers is calculated to be 1% using the formula $(a_{PbTiO_3}-a_{SrTiO_3})/a_{SrTiO_3}$. For thin layers such strain can be accommodated through elastic distortion, rather than being relaxed through the formation of dislocations. This compressive lattice strain in the cubic $PbTiO_3$ layers is maintained until the specimen is cooled to T_C (490 °C for bulk $PbTiO_3$).[12] When the cubic $PbTiO_3$ transforms to tetragonal $PbTiO_3$ at T_C, compressive strain within the $PbTiO_3$ layer leads to a matching of the *a*-axis of the tetragonal $PbTiO_3$ with the *a*-axis of $SrTiO_3$ in order to minimize strain energy. At room temperature, the magnitude of the lattice strain between the *a* axis of $SrTiO_3$ ($a=3.905$ Å)[21] and $PbTiO_3$ is less than 0.1%, whereas that between the *a* axis of $SrTiO_3$ and *c* axis of $PbTiO_3$ is 6.3%, leading to an energetic preference of the observed orientation. We note that this analysis is based on bulk lattice constants and realize that there may be deviations in the properties of ultrathin $PbTiO_3$ layers (e.g., T_C, equilibrium lattice constants, ferroelectric properties, etc.).

In contrast to $PbTiO_3/SrTiO_3$ superlattices prepared using a sol-gel method in which smeared interfaces and significant interdiffusion were seen,[22] our MBE-grown superlattice is more than an order of magnitude thinner and shows very sharp interfaces. This is clearly shown in the bright-field TEM micrograph in Fig. 3(a) and in the HRTEM image in Fig. 4(a). Furthermore, the structural width of the interface is deduced to be about one unit cell from the measurement of lattice spacings of both $SrTiO_3$ and $PbTiO_3$ in the HRTEM image of the interface shown in Fig. 4(b). It should be pointed out that the chemical width of the interface, which is a measure of atomic diffusion across the superlattice interface, cannot be precisely determined by HRTEM, but may be done using spatially resolved analytical electron microscopy.

In conclusion, high quality $PbTiO_3$ layers and a $PbTiO_3/SrTiO_3$ superlattice were grown on (001) $SrTiO_3$ by reactive MBE. The thin $PbTiO_3$ layers are single crystalline with the [001] direction parallel to the growth direction. The interfaces between $PbTiO_3$ and $SrTiO_3$ in this metastable superlattice are extremely sharp. Such interfacial abruptness and layer thickness control are comparable with what has been achieved in the growth of metastable compound semiconductor superlattices[23,24] and is desired for studying predictions of enhanced dielectric performance in nanoscale dielectric and ferroelectric superlattices.[8,9]

We gratefully acknowledge the financial support of the College of Engineering at the University of Michigan and the Department of Energy through Grant No. DE-FG02-97ER45638. C.D.T. gratefully acknowledges the support of the IMAPS Educational Foundation.

[1] K. Iijima, T. Terashima, Y. Bando, K. Kamigaki, and H. Terauchi, J. Appl. Phys. **72**, 2840 (1992).
[2] T. M. Shaw, A. Gupta, M. Y. Chern, P. E. Batson, R. B. Laibowitz, and B. A. Scott, J. Mater. Res. **9**, 2566 (1994).
[3] I. Kanno, S. Hayashi, R. Takayama, and T. Hirao, Appl. Phys. Lett. **68**, 328 (1996).
[4] H.-M. Christen, L. A. Boatner, J. D. Budai, M. F. Chisholm, L. A. Géa, P. J. Marrero, and D. P. Norton, Appl. Phys. Lett. **68**, 1488 (1996).
[5] E. D. Specht, H.-M. Christen, D. P. Norton, and L. A. Boatner, Phys. Rev. Lett. **80**, 4317 (1998).
[6] H.-M. Christen, E. D. Specht, D. P. Norton, M. F. Chisholm, and L. A. Boatner, Appl. Phys. Lett. **72**, 2535 (1998).
[7] H.-M. Christen, L. A. Knauss, and K. S. Harshavardhan, Mater. Sci. Eng., B **56**, 200 (1998).
[8] N. A. Pertsev, G. Arlt, and A. G. Zembilgotov, Phys. Rev. Lett. **76**, 1364 (1996).
[9] S. Li, J. A. Eastman, J. M. Vetrone, R. E. Newnham, and L. E. Cross, Philos. Mag. B **76**, 47 (1997).
[10] J. V. Mantese, N. W. Schubring, A. L. Micheli, and A. B. Catalan, Appl. Phys. Lett. **67**, 721 (1995).
[11] J. V. Mantese, N. W. Schubring, A. L. Micheli, A. B. Catalan, M. S. Mohammed, R. Naik, and G. W. Auner, Appl. Phys. Lett. **71**, 2047 (1997).
[12] Landolt-Bornstein: *Numerical Data and Functional Relationships in Science and Technology*, New Series, Group III, Vol. 16a, edited by K.-H. Hellwege and A. M. Hellwege (Springer, Berlin, 1981), pp. 77–81.
[13] T. Ikeda, J. Phys. Soc. Jpn. **14**, 1286 (1959).
[14] C. D. Theis and D. G. Schlom, J. Cryst. Growth **174**, 473 (1997).
[15] J. H. Haeni, C. D. Theis, and D. G. Schlom, Mater. Sci. Eng., B (submitted).
[16] C. D. Theis, J. Yeh, D. G. Schlom, M. E. Hawley, and G. W. Brown, Thin Solid Films **325**, 107 (1998).
[17] M. Kawasaki, K. Takahashi, T. Maeda, R. Tsuchiya, M. Shinohara, O. Ishiyama, T. Yonezawa, M. Yoshimoto, and H. Koinuma, Science **266**, 1540 (1994).
[18] J. B. Nelson and D. P. Riley, Proc. Phys. Soc. London **57**, 160 (1945).
[19] Y. Gao, G. Bai, K. L. Merkle, Y. Shi, H. L. M. Chang, Z. Shen, and D. J. Lam, J. Mater. Res. **8**, 145 (1993).
[20] S. G. Ghonge, E. Goo, and R. Ramesh, Appl. Phys. Lett. **62**, 1742 (1993).
[21] D. Taylor, Trans. J. Br. Ceram. Soc. **84**, 181 (1985).
[22] Y. Ohya, T. Ito, and Y. Takahashi, Jpn. J. Appl. Phys., Part 1 **33**, 5272 (1994).
[23] A. K. Gutakovskii, L. I. Fedina, and A. L. Aseev, Phys. Status Solidi A **150**, 127 (1995).
[24] S. Thoma and H. Cerva, Ultramicroscopy **53**, 37 (1994).